

## RESEARCH ARTICLE

10.1002/2016PA002968

## Key Points:

- Spatially variable correlations between Li/Mg and Sr/Ca ratios and temperature in *Siderastrea siderea*
- Downcore coral skeletal Li/Mg and Sr/Ca ratios are well correlated with HadISST in the forereef
- Li/Mg is a useful addition to the SST proxy toolbox in some regions

## Supporting Information:

- Supporting Information S1
- Table S1
- Table S2
- Table S3
- Table S4
- Table S5

## Correspondence to:

S. E. Fowell,  
s.fowell@noc.soton.ac.uk

## Citation:

Fowell, S. E., K. Sandford, J. A. Stewart, K. D. Castillo, J. B. Ries, and G. L. Foster (2016), Intrareef variations in Li/Mg and Sr/Ca sea surface temperature proxies in the Caribbean reef-building coral *Siderastrea siderea*, *Paleoceanography*, 31, 1315–1329, doi:10.1002/2016PA002968.

Received 19 APR 2016

Accepted 15 SEP 2016

Accepted article online 19 SEP 2016

Published online 5 OCT 2016

©2016. The Authors.

This is an open access article under the terms of the Creative Commons Attribution License, which permits use, distribution and reproduction in any medium, provided the original work is properly cited.

# Intrareef variations in Li/Mg and Sr/Ca sea surface temperature proxies in the Caribbean reef-building coral *Siderastrea siderea*

Sara E. Fowell<sup>1</sup>, Kate Sandford<sup>1</sup>, Joseph A. Stewart<sup>1,2</sup>, Karl D. Castillo<sup>3</sup>, Justin B. Ries<sup>4</sup>, and Gavin L. Foster<sup>1</sup>

<sup>1</sup>Ocean and Earth Science, National Oceanography Centre, University of Southampton, Southampton, UK, <sup>2</sup>Hollings Marine Laboratory, National Institute of Standards and Technology, Charleston, South Carolina, USA, <sup>3</sup>Department of Marine Sciences, University of North Carolina at Chapel Hill, Chapel Hill, North Carolina, USA, <sup>4</sup>Marine Science Center, Northeastern University, Nahant, Massachusetts, USA

**Abstract** Caribbean sea surface temperatures (SSTs) have increased at a rate of 0.2°C per decade since 1971, a rate double that of the mean global change. Recent investigations of the coral *Siderastrea siderea* on the Belize Mesoamerican Barrier Reef System (MBRS) have demonstrated that warming over the last 30 years has had a detrimental impact on calcification. Instrumental temperature records in this region are sparse, making it necessary to reconstruct longer SST records indirectly through geochemical temperature proxies. Here we investigate the skeletal Sr/Ca and Li/Mg ratios of *S. siderea* from two distinct reef zones (forereef and backreef) of the MBRS. Our field calibrations of *S. siderea* show that Li/Mg and Sr/Ca ratios are well correlated with temperature, although both ratios are 3 times more sensitive to temperature change in the forereef than in the backreef. These differences suggest that a secondary parameter also influences these SST proxies, highlighting the importance for site- and species-specific SST calibrations. Application of these paleothermometers to downcore samples reveals highly uncertain reconstructed temperatures in backreef coral, but well-matched reconstructed temperatures in forereef coral, both between Sr/Ca-SSTs and Li/Mg-SSTs, and in comparison to the Hadley Centre Sea Ice and Sea Surface Temperature record. Reconstructions generated from a combined Sr/Ca and Li/Mg multiproxy calibration improve the precision of these SST reconstructions. This result confirms that there are circumstances in which both Li/Mg and Sr/Ca are reliable as stand-alone and combined proxies of sea surface temperature. However, the results also highlight that high-precision, site-specific calibrations remain critical for reconstructing accurate SSTs from coral-based elemental proxies.

## 1. Introduction

Global mean sea surface temperatures (SSTs) have been rising since the Industrial Revolution, primarily as a result of the change in the radiative forcing imposed by increasing anthropogenic greenhouse gas emissions (e.g., atmospheric  $p\text{CO}_2$  change from 280 to 400 ppm [Cubasch *et al.*, 2013]). The atmosphere carries only 2% of the heat content of the ocean-atmosphere system, and in tandem with an increase in atmospheric temperature, the global average warming in the upper 75 m of the oceans has been 0.11°C per decade (between 1971 and 2010). This global SST increase is not geographically uniform and is amplified in areas such as the Caribbean Sea, where it has increased at a rate of more than 0.2°C per decade, resulting in a total change of ~0.8°C over the last 40 years [Rhein *et al.*, 2013; Glenn *et al.*, 2015].

Valuable insight into the impacts of future SST changes on areas of ecological importance, such as coral reefs, can be obtained from the response of ecosystems to past environmental change. Yet historical records of SST prior to the period of modern instrumentation (1970s) are based on relatively sporadic measurements acquired by using a wide range of SST monitoring techniques including buckets, shipboard sensors, floating buoys, and satellites. These techniques have differing accuracies, precisions, and sampling depths, leading to relatively large uncertainties and anomalies within the historical records [Smith *et al.*, 2008; Kennedy *et al.*, 2011]. Geochemical proxy reconstructions of SSTs therefore provide an attractive alternative to the intermittent in situ monitoring data sets and a means to potentially extend SST records well beyond that of the instrumental monitoring period [Tierney *et al.*, 2015]. To this end, a number of biogenic substrates have been utilized for geochemical proxy SST reconstruction including organic material such as alkenones [Brassell *et al.*, 1986] and membrane lipids of marine Crenarchaeota [Schouten *et al.*, 2002], as well as the calcium

carbonate skeletons of marine organisms such as planktonic foraminifera [Anand et al., 2003], sclerosponges [Rosenheim et al., 2004], and tropical corals [Beck et al., 1992; de Villiers et al., 1994; Alibert and McCulloch, 1997; Swart et al., 2002; Reynaud et al., 2007; Maupin et al., 2008; Mitsuguchi et al., 2008; DeLong et al., 2014]. Of these possible archives for SST estimates, only the skeletons of tropical corals offer the fine-scale temporal resolution and long growth histories necessary to resolve SST changes over the last ~300 years at an interannual resolution [Anderson et al., 2013].

Corals are used as paleothermometers because the partition coefficients between seawater and coral aragonite ( $K_D = (X/Ca)_{\text{coral}} / (X/Ca)_{\text{sw}}$ ) of various auxiliary cations such as  $\text{Li}^+$  [Marriott et al., 2004a],  $\text{Mg}^{2+}$  [Mitsuguchi et al., 1996], and  $\text{Sr}^{2+}$  [Beck et al., 1992] are understood to be temperature-dependent. These ions are transported from seawater to the semi-isolated extracellular calcifying fluid [Sinclair and Risk, 2006; Gaetani et al., 2011; Tambutti et al., 2011; Gagnon et al., 2012] by direct diffusion [Cohen et al., 2006; Gaetani and Cohen, 2006; Gagnon et al., 2007, 2012] or by active transport [Ip and Lim, 1991; Ferrier-Pagès et al., 2002].  $\text{Sr}^{2+}$  ions are thought to replace  $\text{Ca}^{2+}$  ions in the aragonite lattice due to their similar ionic radii (1.31 Å and 1.18 Å, respectively [Shannon, 1976; Watson, 1996; Allison et al., 2005]). However, it is argued that the ionic radii of  $\text{Mg}^{2+}$  and  $\text{Li}^+$  (0.89 Å and 0.92 Å, respectively [Shannon, 1976]) are too small to directly substitute for  $\text{Ca}^{2+}$  [Finch and Allison, 2008; Montagna et al., 2014]. Nonetheless, while the incorporation pathways remain debated, the similar ionic sizes and partition coefficients ( $K_D \ll 1$ ) for both  $\text{Mg}^{2+}$  and  $\text{Li}^+$ , and the positive correlation between Mg/Ca and Li/Ca ratios in coral [Montagna et al., 2014], provide evidence that similar processes govern their incorporation into coral aragonite [Case et al., 2010; Hathorne et al., 2013b; Raddatz et al., 2013; Montagna et al., 2014].

The Sr/Ca ratio is the most commonly used geochemical temperature proxy in coral archives [e.g., Weber, 1973; Beck et al., 1992; de Villiers et al., 1994; McCulloch et al., 1994; Alibert and McCulloch, 1997; Cohen et al., 2001, 2002; Ferrier-Pagès et al., 2002; Swart et al., 2002; Fallon et al., 2003; Gagnon et al., 2007; Reynaud et al., 2007; Maupin et al., 2008; Mitsuguchi et al., 2008; Caroselli et al., 2012; Gagan et al., 2012; Gagnon et al., 2013; Raddatz et al., 2013; DeLong et al., 2014]. However, the reliability of this proxy has been recently called into question. For instance, the sensitivity of Sr/Ca to temperature change differs among and between coral species, and relative to inorganically precipitated aragonite [e.g., Cohen et al., 2006; Corrège, 2006], suggesting that species- and even colony-specific calibrations are needed [e.g., Alpert et al., 2016].

The lack of a robust universal Sr/Ca-SST calibration for a single species of coral, or even different individuals within the same colony, is well demonstrated [Corrège, 2006; Saenger et al., 2008; Gaetani et al., 2011]. Such intercolonial and intracolonial variations may arise from factors other than the temperature influence on the Sr/Ca ratio of coral skeletons. For example, some studies identify a mineralogical/microstructural control such as crystal shape and location within the skeletal microstructure [Cohen et al., 2001; Meibom et al., 2006; Raddatz et al., 2013] and the influence of kinetic processes such as calcification rate [Cohen et al., 2001; Gaetani and Cohen, 2006]. An additional complicating factor for Sr/Ca and all element to calcium ratios in biogenic carbonates is Rayleigh fractionation that occurs during the precipitation of ions from a semi-isolated batch of calcifying fluid, which is only periodically replenished by the diffusion of ions from seawater [Gaetani and Cohen, 2006]. The extent to which Rayleigh fractionation affects a particular elemental ratio depends on the partition coefficient ( $K_D$ ) that is itself temperature-dependent [Gaetani and Cohen, 2006]. For example, as temperature increases from 5°C to 30°C, the  $K_D^{\text{Sr/Ca}}$  for inorganic aragonite decreases by 14% [Gaetani et al., 2011], resulting in fewer Sr ions becoming incorporated into the carbonate matrix. In aragonite, the  $K_D$  of Li/Ca and Mg/Ca also exhibits an inverse relationship with temperature [Marriott et al., 2004b; Gaetani et al., 2011]. Rayleigh fractionation influences the composition of an isolated fluid undergoing partial crystallization when the  $K_D$  of the participating elements is not equal to 1. As  $\text{CaCO}_3$  is precipitated, the concentration of Ca in the calcifying fluid decreases, causing the concentration of other elements with a  $K_D < 1$  to increase relative to Ca (and vice versa). The elemental composition of coral aragonite in terms of element-to-calcium ratio is therefore determined by the  $K_D$  of each element, its relationship with temperature, and the amount of Ca precipitated from each batch of calcifying fluid [Cohen et al., 2006; Gaetani and Cohen, 2006; Gagnon et al., 2007; Montagna et al., 2014].

These complicating factors associated with coral Sr/Ca have prompted a search for alternative SST proxies, such as Li/Mg ratios [Case et al., 2010; Hathorne et al., 2013b; Raddatz et al., 2013; Montagna et al., 2014]. The potential of the Li/Mg-SST proxy lies in the opposing temperature controls on Li/Ca and Mg/Ca in the

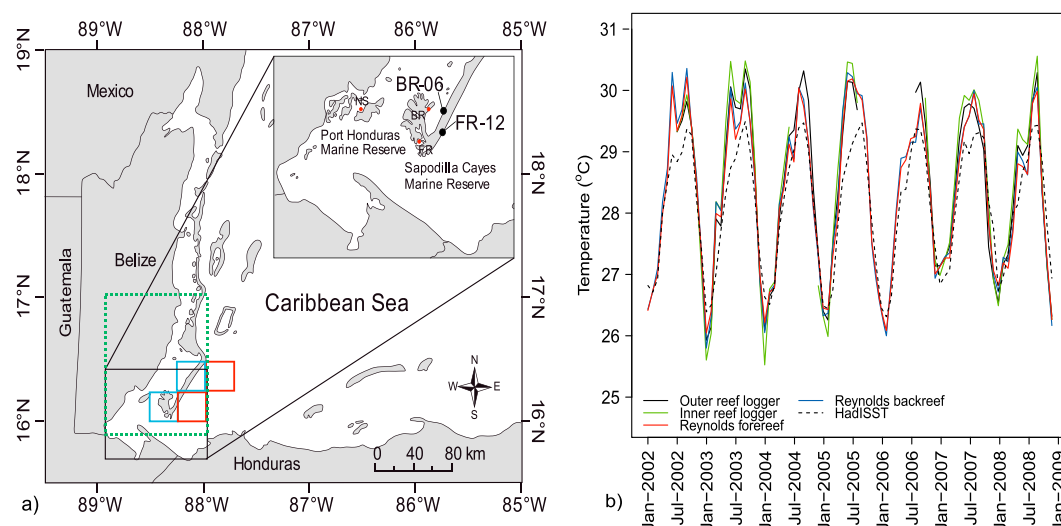


**Figure 1.** Coral core and temperature data locations in southern Belize. (a) The  $0.25^{\circ} \times 0.25^{\circ}$  grids represent the areas covered by the Reynolds forereef (red) and backreef (blue) temperature data. The red circles show the location of the temperature loggers, with the nearshore logger representing the inner reef, and the forereef and backreef representing the outer reef. The  $1^{\circ} \times 1^{\circ}$  green dashed box represents the area covered by the HadISST satellite temperature data. BR-06 and FR-12 are the sampling locations of the forereef FR-12 and backreef BR-06 cores, respectively, which were analyzed in the present study. (b) Monthly resolved temperature data from the outer reef in situ logger (black), inner reef in situ logger (green), Reynolds forereef composite (red), Reynolds backreef composite (blue), and HadISST data (dashed).

coral skeleton, thereby amplifying the effect of temperature on Li/Mg, and the similar responses of these ratios to Rayleigh fractionation, meaning that precipitation progress does not have a significant influence on the Li/Mg ratio of the calcifying fluid [Montagna *et al.*, 2014]. Li and Mg incorporation into aragonite is therefore, in theory at least, simply reliant on the temperature-dependent partition coefficients of Li and Mg, rather than on the extent of Rayleigh fractionation. Several recent studies have confirmed a strong temperature dependence for Li/Mg ratios in corals, which appears to be relatively insensitive to the species used [Montagna *et al.*, 2014, and references therein]. Use of the first multispecies Li/Mg-SST calibration permits reconstruction of SSTs with an uncertainty of  $\pm 1.8^{\circ}\text{C}$  (at 95% confidence [Montagna *et al.*, 2014]), an improvement on the uncertainties associated with the *Porites*-only Li/Mg-SST calibrations [Hathorne *et al.*, 2013b].

Here we present new Li/Mg and Sr/Ca data from the previously unexamined coral species *Siderastrea siderea* sampled from the Caribbean Sea (Belize), which allow us to place this taxa in the broader context of other, tropical coral species utilized for SST reconstruction, such as *Porites* [Hathorne *et al.*, 2013b]. Additionally, we examine the use of multiproxy calibrations to test whether combining elemental ratios with strong temperature dependencies improves the reliability of SST reconstructions. These detailed calibrations of SST proxies in the coral *S. siderea* allow us to assess the robustness of these proxies in characterizing the extent of ocean warming in the ecologically vulnerable region of the southern Mesoamerican Barrier Reef System.

## 2. Methodology

### 2.1. Sample Collection

In February 2009, coral cores were collected from the forereef and backreef in the Sapodilla Cayes Marine Reserve (southern Belize; western Caribbean Sea). A full description of the core extraction and sectioning methods is available in Castillo *et al.* [2011]. The cores analyzed in this study were FR-12 ( $16.10004^{\circ}\text{N}$ ,  $88.26669^{\circ}\text{W}$ ) and BR-06 ( $16.14045^{\circ}\text{N}$ ,  $88.26015^{\circ}\text{W}$ ; Figure 1a).

### 2.2. Temperature Data

High temporal resolution in situ temperature measurements from the study site were acquired from 2002 to 2008 by using Hobo (Onset, Massachusetts) temperature loggers (Figure 1 and Table S1 in the supporting information) [Castillo and Lima, 2010]. These data were augmented by Reynolds SST data from paired  $0.25^{\circ}$  latitude/longitude sized grids (Figure 1 and Table S1; <http://www.nhc.noaa.gov/sst/>) to account for

incompleteness in the in situ logger records. Reynolds SSTs were found to be strongly correlated with the in situ SST measurements and are therefore representative of the temperature regimes experienced by the investigated corals [Reynolds *et al.*, 2007; Castillo and Lima, 2010; Castillo *et al.*, 2012]. No significant difference was found between the temperatures experienced in the two coral reef zones, either in the Reynolds data set ( $p = 0.86$ ) or the temperature loggers ( $p = 0.89$ ) of Castillo and Lima [2010].

The in situ temperature reconstructions were compared to the Hadley Centre Sea Ice and Sea Surface Temperature Version 1 (HadISST1) [Rayner *et al.*, 2003] historic temperature record for this location (16–17°N, 88–87°W). HadISST is a global SST product with  $1^\circ \times 1^\circ$  resolution grids and monthly temperature records from January 1870 to present (<http://climexp.knmi.nl>; Table S1). Grid points that are missing satellite data within the HadISST data set were statistically interpolated from adjacent grids [Rayner *et al.*, 2006]. Although the overall forereef and backreef Reynolds composites do not differ significantly from HadISST ( $p = 0.26$  and  $p = 0.20$ , respectively), the summer temperatures are frequently lower in the HadISST record, with the Reynolds-derived summer temperatures being on average 0.41°C higher for the forereef and 0.44°C higher for the backreef (both with  $p < 0.01$ ).

### 2.3. Sample Preparation and Analysis

#### 2.3.1. Monthly Resolution Subsampling

Coral slabs (70 × 45 × 5 mm) were X-rayed by using a *Fuji Computed Radiography* radiography system at the University of North Carolina at Chapel Hill Campus Health Services Radiology Department, at 6 mA s<sup>−1</sup> and 40 kV. These images were used to calculate an annual chronology by labeling the first high-density band (deposited the same winter as the collection) and counting each subsequent high-density band backward in time.

Slabs from FR-12 and BR-06 were sampled at monthly to bimonthly resolution from the top (September 2008 to January 2006 and September 2008 to February 2006, respectively) and bottom (November 1921 to December 1925 and November 1922 to January 1926, respectively) of each coral slab (Figure 2). A New Wave Research micromill with a 500 μm diameter diamond drill bit was used to drill ~1 mm wide trenches to a depth of 1 mm in the thecal wall (Figure 2), using a protocol similar to that of DeLong *et al.* [2011]. The widths of the thecal walls were identified under the microscope to minimize the chance of sampling the columella. Sample sizes ranged from 0.3 to 1.4 mg.

Final age models were built for the field calibrations following a standard approach [e.g., Felis *et al.*, 2004; Maupin *et al.*, 2008; Felis *et al.*, 2009]. A preliminary age range was estimated by counting annual high-density bands (Figures 2a and 2c). Then, this annually resolved age model, the coral age at collection, the skeletal location of the first monthly sample, and subsequent peaks and troughs in the Sr/Ca ratio were used to identify warm and cold intervals in the SST time series, assuming the inverse relationship between Sr/Ca and SST seen in other studies [Maupin *et al.*, 2008; DeLong *et al.*, 2011, 2014]. A polynomial curve was fit through 6 depth-age points allowing the age at each sample depth to be predicted. Instrumental SST was then interpolated on to this coral age scale to permit direct comparison of temperature records.

Downcore samples from FR-12 (1921–1925) and BR-06 (1922–1926) were dated by counting the annual density bands on the X-ray images (Figures 2b and 2d). To determine the exact months, a method similar to that of Maupin *et al.* [2008] was used whereby the summer and winter peaks from the reconstructed SSTs were tied to the monthly resolved Hadley Centre's HadISST gridded temperature data set for the corresponding year.

#### 2.3.2. Cleaning Procedure

Residual organic matter removal protocols are derived from foraminiferal calcite oxidative cleaning techniques and following the standard protocol of Henehan *et al.* [2013], originally described by Barker *et al.* [2003]. Micromill extracted CaCO<sub>3</sub> powders were oxidatively cleaned in 250–500 μL of 1% H<sub>2</sub>O<sub>2</sub> (buffered in 0.1 M NH<sub>4</sub>OH<sub>4</sub>) at 80°C for a total of 15 min with intermittent ultrasonication. The spent oxidative mixture was removed, and samples were thoroughly rinsed by using 18.2 MΩ Milli-Q water. Between each subsequent rinse step, the powdered samples were centrifuged for 2 min (13,000 rpm) to minimize sample loss. Samples were then transferred into acid-cleaned microcentrifuge tubes before a weak acid (0.0005 M HNO<sub>3</sub>) leach was performed to remove any ions readsorbed onto the sample surface. Samples were then dissolved in the minimum volume of 0.5 M HNO<sub>3</sub>. Dissolved sample solutions were finally centrifuged for 3 to 5 min (13,000 rpm) and transferred into clean vials to separate the supernatant from any remaining noncarbonate solids.



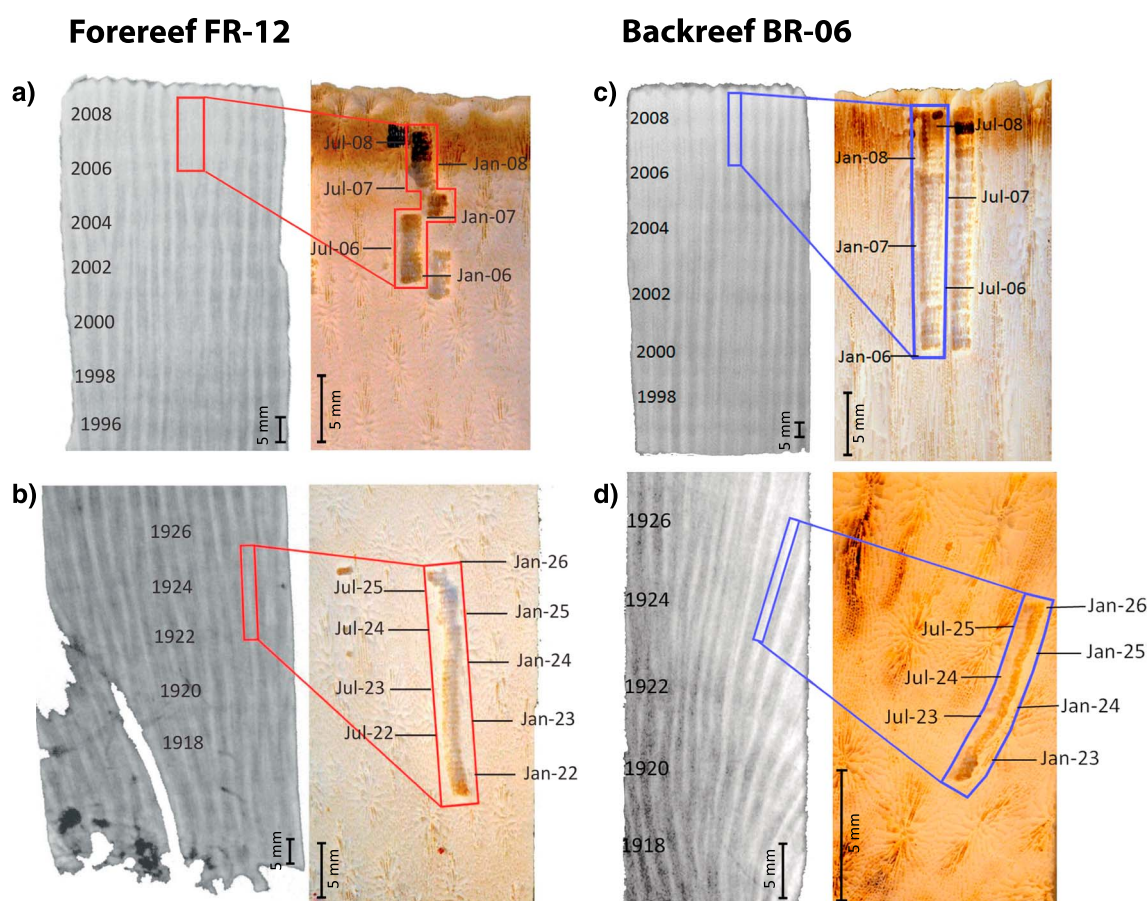


**Figure 2.** Coral slab X-rays with annual bands labeled. The rectangles indicate where the coral was subsampled along the high-density theca wall (bright vertical bands). Optical images after subsampling are labeled with the position of the January and July samples. Theca walls are identified by a smoother, less porous appearance. (a) Top of the forereef FR-12 coral. (b) Downcore FR-12. (c) Top of the backreef BR-06 coral. (d) Downcore BR-06.

### 2.3.3. Inductively Coupled Plasma–Mass Spectrometry Analysis

All analyses were carried out at the University of Southampton (UK). Calcium concentrations of the dissolved samples were first determined by using quadrupole inductively coupled plasma–mass spectrometry (ICP-MS; Thermo Scientific X-Series), giving an estimate of the major elemental composition of the dissolved samples in order to accurately matrix match for subsequent quantitative multielemental analysis. X-Series standards and samples were made by using 3%  $\text{HNO}_3$  spiked with 5 ppb In, 5 ppb Re, and 20 ppb Be, which act as internal standards to monitor drift and correct for mass bias in the absence of bracketing standards. A multielement standard stock solution made by using high-concentration (10,000 ppm) single element (B, Mg, Al, Sr, and Ca) solutions was diluted to make four gravimetric standards with differing Ca concentrations (0.2 to 3 ppm Ca). To monitor the accuracy and precision of the measurements, consistency standards of 1 ppm, 3 ppm, and 7 ppm Ca CS2 and CS3 [Ni, 2006; Ni *et al.*, 2007] were analyzed at the beginning and end of each analytical session. Based on these analyses, the external precision at  $1\sigma$  was estimated to be  $\pm 1.01\%$  for 1 ppm Ca,  $\pm 4.91\%$  for 3 ppm Ca, and  $\pm 4.94\%$  for 7 ppm Ca.

An Element XR (Thermo Scientific) sector field ICP-MS was used to determine the element to Ca ratios of the coral dissolutions. A suite of element intensity ratios (including Li/Ca, B/Ca, Mg/Ca, and Sr/Ca) were measured to determine the skeletal elemental composition of the samples and also the efficacy of sample cleaning (e.g.,  $\text{Al/Ca} < 100 \mu\text{mol/mol}$  indicative of minimal clay mineral contamination). Further information regarding the measurement of Li can be found in Text S1 and Figure S1 in the supporting information [Al-Ammar *et al.*, 2000; Ni, 2006]. Samples were analyzed in batches of equal Ca concentrations between 1 mM and 3 mM and blank corrected with a 0.5 M  $\text{HNO}_3$  “blank” measured between every sample/standard [Rosenthal *et al.*, 1999]. Each block of three samples was bracketed against a matrix-matched (i.e., of equal Ca concentration

**Table 1.** Comparison of JCp-1 Elemental Ratios Measurements<sup>a</sup>

	This Study	Interlab Comparison	Hathorne <i>et al.</i> [2013b]	Montagna <i>et al.</i> [2014]
Sr/Ca mmol/mol average	8.66 ( <i>n</i> = 20)	8.84 ( <i>n</i> = 179)		
Standard deviation	0.10	0.04		
External precision (%) <sup>b</sup>	2.21	0.95 <sup>c</sup>		
Li/Mg mmol/mol average	1.51 ( <i>n</i> = 16)	1.48 ( <i>n</i> = 5)	1.51 ( <i>n</i> = 25)	1.43
Standard deviation	0.03	0.06	0.04	
External precision (%) <sup>b</sup>	4.45	7.43	5.30	3.20

<sup>a</sup>Long-term precision is determined by repeat JCp-1 measurements, which are compared with the recent Li/Mg studies of Hathorne *et al.* [2013b] and Montagna *et al.* [2014] in addition to the international laboratory comparison [Hathorne *et al.*, 2013a].

<sup>b</sup>External precision reported as 2 relative standard deviations.

<sup>c</sup>Median interlab external precision is 0.28%.

to the samples [Rosenthal *et al.*, 1999]), well-characterized, gravimetric standard solution (prepared by Cardiff University). Sample ratios were calculated by calibrating to the standard solution, which had values of 11.38  $\mu\text{mol/mol}$ , 2.44 mmol/mol, and 1.43 mmol/mol for Li/Ca, Mg/Ca, and Sr/Ca respectively, allowing samples to be corrected for instrumental and matrix-induced mass bias.

Additionally, three consistency standards (SECS1, SECS2, and SECS3; University of Southampton) of matching [Ca] but different gravimetrically prepared and cross-calibrated elemental ratios (Table S2) were used as internal standards to monitor accuracy and thus efficiency of correcting for mass bias effects and instrumental drift. Using the bracketing standards method, precise values of repeat measurements were obtained for these standards. SECS3 is the most similar in composition to the coral samples and yielded average measured values ( $2\sigma$ ) for Sr/Ca of  $1.97 \pm 0.04$  mmol/mol and Li/Mg of  $5.51 \pm 0.09$  mmol/mol compared to 2 mmol/mol and 5.73 mmol/mol, respectively, determined gravimetrically (Table S2).

Alongside each batch of ~15 coral samples, a JCp-1 standard (international coral reference material made from homogenized *Porites* [Okai *et al.*, 2002]) was analyzed in the same manner as the coral samples in this study (1 to 2 mg JCp-1). Replicates of JCp-1 passed through the entire sample cleaning and analytical protocol provide a rigorous assessment of true external precision. The average JCp-1 values and standard deviation during the course of this study are shown in Table 1. While Li/Mg measurements of JCp-1 for this study are comparable to those of other laboratories, our mean Sr/Ca value is at the low end of the range of values in the Hathorne *et al.* [2013a] interlaboratory study (Table 1). By comparing analyses of cleaned and uncleaned samples of JCp-1, we found that both Li/Ca and Mg/Ca ratios decreased by 25% as a result of the removal of organic matter (Figure S2), a similar result to that observed in foraminiferal calcite Mg/Ca following oxidative cleaning [Barker *et al.*, 2003]. In contrast, both Sr/Ca and Li/Mg ratios are shown to be relatively unaffected by this sample cleaning procedure (Text S2 and Figure S2), the latter due to a precisely equal reduction in [Mg] and [Li]. Further details about the cleaning test can be found in the supporting information [Ni, 2006; Ni *et al.*, 2007].

## 2.4. Data Handling

### 2.4.1. Statistical Analysis

The statistical software package R Studio [R Development Core Team, 2013] was used for all data analysis and for constructing linear regression models on measured Li/Mg and Sr/Ca data. The uncertainty of the temperature estimates using the linear regression models was assessed by using 95% prediction intervals. Welch unequal variance two sample *t* tests (two-tailed) were also used to determine whether there were significant differences between mean summer or winter temperatures between reconstructed temperatures and the historic HadISST record.

### 2.4.2. Data Compilations

A “multispecies” Li/Mg-T calibration of cold-water, temperate, and tropical coral species was developed by using the data from this study and solution ICP-MS data from previous studies [Case *et al.*, 2010; Hathorne *et al.*, 2013b; Raddatz *et al.*, 2013; Montagna *et al.*, 2014]. Based on a consideration of the long-term average of JCp-1 at the University of Southampton, Li/Mg results from Montagna *et al.* [2014] were increased by 5% to make them comparable with the results of the present study (Table 1).

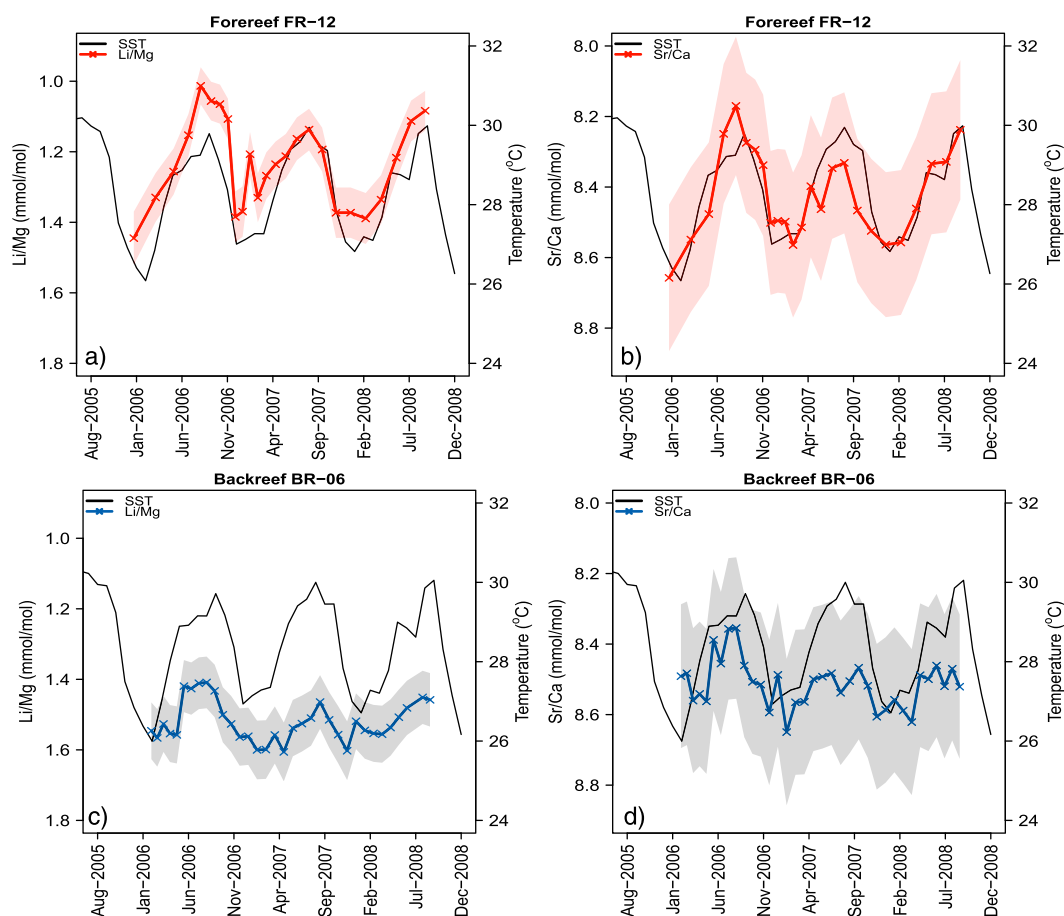


**Figure 3.** Monthly resolved Li/Mg and Sr/Ca ratios in forereef FR-12 (red) and backreef BR-06 (blue) samples. The crosses represent the ICP-MS measured data with  $2\sigma$  external reproducibility shown as a shaded band. Reynolds composite temperature records are shown in black for comparison.

### 3. Results

#### 3.1. Monthly Resolved Sr/Ca and Li/Mg Ratios

Geochemical coral data (Table S3) are compared to composite observational temperature data (Table S1) in Figure 3. Both the Li/Mg and Sr/Ca ratios in the forereef coral FR-12 (Figures 3a and 3b) demonstrate a strong seasonal cycle in step with observed intraannual temperature fluctuations. Similar, but smaller-amplitude cycles, are also present in the backreef coral BR-06 (Figures 3c and 3d). In both corals, these elemental ratios are higher during colder months, demonstrating that both Li/Mg and Sr/Ca ratios exhibit typical inverse relationships with temperature.

#### 3.2. Calibrations

Simple linear regressions reveal that the Li/Mg ratio of the forereef coral FR-12 has the best defined correlation with more than 70% of variation explained by temperature ( $r^2 = 0.71$ ,  $p \ll 0.01$ ; Figure 4a), as opposed to only 40% explained by temperature in the backreef coral BR-06 ( $r^2 = 0.40$ ,  $p \ll 0.01$ ; Figure 4c). The Sr/Ca ratio is also better correlated with temperature in the forereef coral FR-12 ( $r^2 = 0.69$ ,  $p \ll 0.01$ ; Figure 4b) than in the backreef BR-06 coral ( $r^2 = 0.26$ ,  $p \ll 0.01$ ; Figure 4d). These relationships between elemental ratios and temperature are also summarized in Table 2.

Stronger correlations the forereef calibrations result in more precise SST reconstructions than for the backreef calibrations and, independent of elemental ratios, lower reconstruction uncertainties are associated with the forereef samples (Table 2).

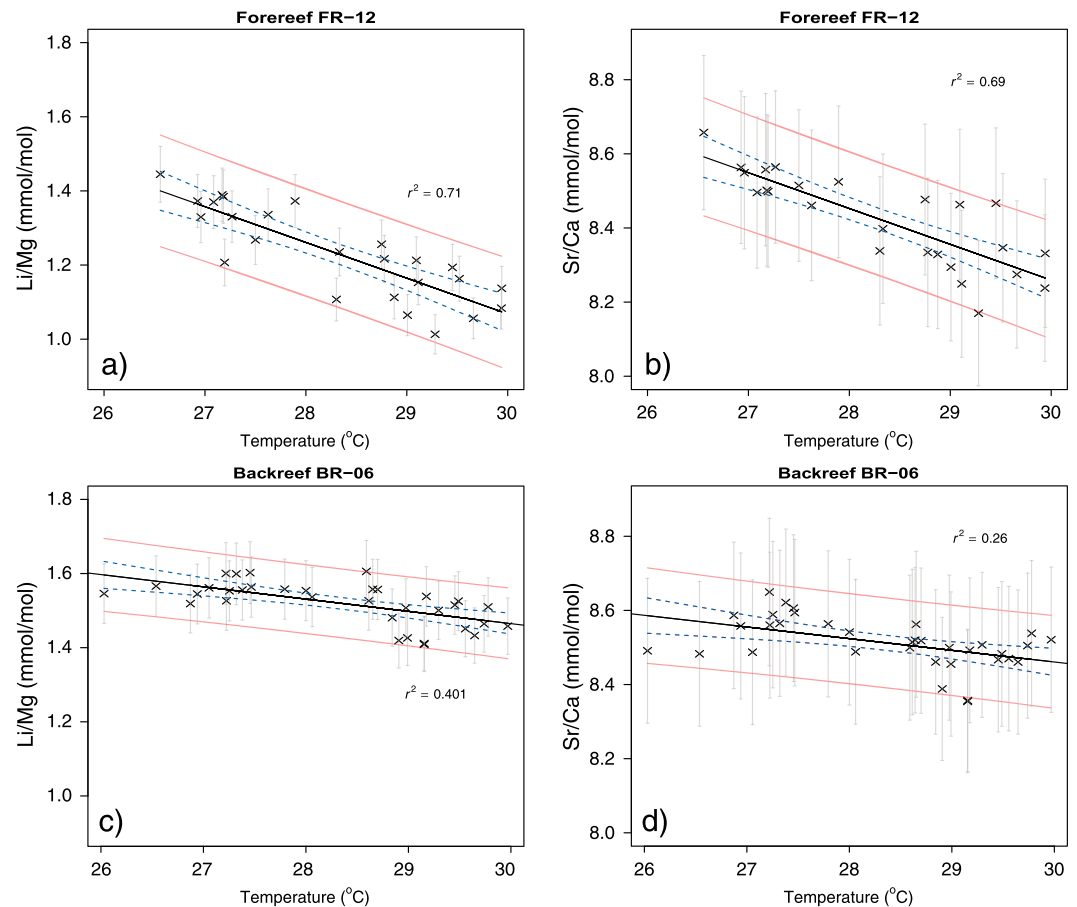


**Figure 4.** Forereef and backreef field-based calibrations of Sr/Ca and Li/Mg temperature proxies in *Siderastrea siderea*. The crosses indicate the individual samples with  $2\sigma$  external reproducibility errors. The blue and red dashed lines show the 95% confidence and prediction intervals, respectively.

Two multiple linear regressions were also performed on the corals to generate multiproxy SST calibrations. The first multiple linear regression combined the Li/Mg and Sr/Ca ratios (hereafter referred to as “MLR1”). The second multiple linear regression combined Li/Ca, Sr/Ca, and Mg/Ca ratios (hereafter referred to as “MLR2”). The regression coefficients for these multiproxy calibrations are shown in Table 3.

The Li/Mg-SST calibrations were added to the existing combined-species calibration described in section 2.4.2 (Figure 5) to generate what will be referred to henceforth as the “multispecies calibration.” The *S. siderea* samples broadly fit the trend of the multispecies calibration of Montagna *et al.* [2014] and extend the upper end of the temperature range by  $\sim 2^\circ\text{C}$ . The backreef data are slightly offset from the curve fitted through the combined data (Figure 5). The resulting exponential equation of the multispecies calibration ( $r^2 = 0.95$ ,  $p \ll 0.001$ ) is

$$\text{Li/Mg} = 5.405 \exp^{(-0.05(\pm 0.001) \times T)} \quad (1)$$

**Table 2.** Regression Statistics for the Forereef and Backreef Calibrations<sup>a</sup>

Calibration	<i>c</i>	$\pm 2$ SE	<i>m</i>	$\pm 2$ SE	$r^2$	<i>p</i>	95% Precision at $28^\circ\text{C}$ ( $^\circ\text{C}$ )
Forereef Li/Mg	3.962	$\pm 0.730$	$-0.097$	$\pm 0.013$	0.71	$<< 0.01$	1.5
Backreef Li/Mg	2.458	$\pm 0.406$	$-0.033$	$\pm 0.007$	0.40	$<< 0.01$	2.7
Forereef Sr/Ca	11.158	$\pm 0.772$	$-0.097$	$\pm 0.014$	0.69	$<< 0.01$	1.6
Backreef Sr/Ca	9.406	$\pm 0.536$	$-0.031$	$\pm 0.009$	0.26	$< 0.01$	4.0

<sup>a</sup>Calibrations in this study were fitted with a linear regression in the form  $\text{Li/Mg} = m \times \text{SST}(^\circ\text{C}) + c$ . Temperature precision estimates were derived from the prediction intervals.



**Table 3.** Multiple Linear Regression Statistics for the Multielemental Forereef and Backreef Calibrations<sup>a</sup>

Calibration	c	x <sub>1</sub>	x <sub>2</sub>	x <sub>3</sub>	x <sub>4</sub>	r <sup>2</sup>	95% Precision at 28°C (°C)
Forereef MLR1	59.854	4.484	3.090	—	—	0.70	1.3
Forereef MLR2	33.177	—	1.205	0.657	2.066	0.75	1.2
Backreef MLR1	54.624	11.115	1.104	—	—	0.36	1.8
Backreef MLR2	38.153	—	0.490	3.466	3.722	0.38	1.8

<sup>a</sup>MLR1 calibrations are in the form  $SST(^{\circ}C) = c - (x_1 \times Li/Mg) - (x_2 \times Sr/Ca)$ . MLR2 calibrations are in the form  $SST(^{\circ}C) = c - (x_3 \times Li/Ca) - (x_2 \times Sr/Ca) + (x_4 \times Mg/Ca)$ . Temperature precision estimates were derived from the prediction intervals.

### 3.3. Downcore Samples and Temperature Reconstructions

Strong seasonal cycles in Li/Mg and Sr/Ca are evident in the forereef and backreef downcore samples (Figure 6 and Table S4). The mean Li/Mg of the forereef coral (1.33 mmol/mol) is significantly lower than that of the backreef coral (1.50 mmol/mol;  $p \ll 0.01$ ). The mean Sr/Ca ratios, however, are not significantly different between reef zones (8.50 mmol/mol and 8.53 mmol/mol in the forereef and backreef, respectively;  $p = 0.27$ ).

Forereef and backreef field-based *S. siderea* calibrations (Table 2) were applied to their respective downcore time series to reconstruct monthly resolved SSTs between 1921 and 1926 (Table S4). In both reef zones the temperature reconstructions using single regressions of Li/Mg and Sr/Ca are within uncertainty ( $2\sigma$ ) of each other, although this is largely a consequence of the propagation of the uncertainty in the backreef calibrations, which are up to  $\pm 12^{\circ}C$  in some instances (Figure 7). Table 4 shows a comparison between the individual SST reconstructions and the HadISST data set. In the forereef, the overall means of both the Li/Mg-SSTs and Sr/Ca-SSTs are within  $0.3^{\circ}C$  of HadISST, and within  $0.7^{\circ}C$  and  $0.1^{\circ}C$  in the summer and winter, respectively, all within calibration uncertainties ( $\pm 1.5^{\circ}C$ ; Table 2). In the backreef, the overall means of the Li/Mg- and Sr/Ca-SSTs are both within  $1.4^{\circ}C$  of HadISST; however, summer Li/Mg-SSTs are  $3.3^{\circ}C$  greater than HadISST and

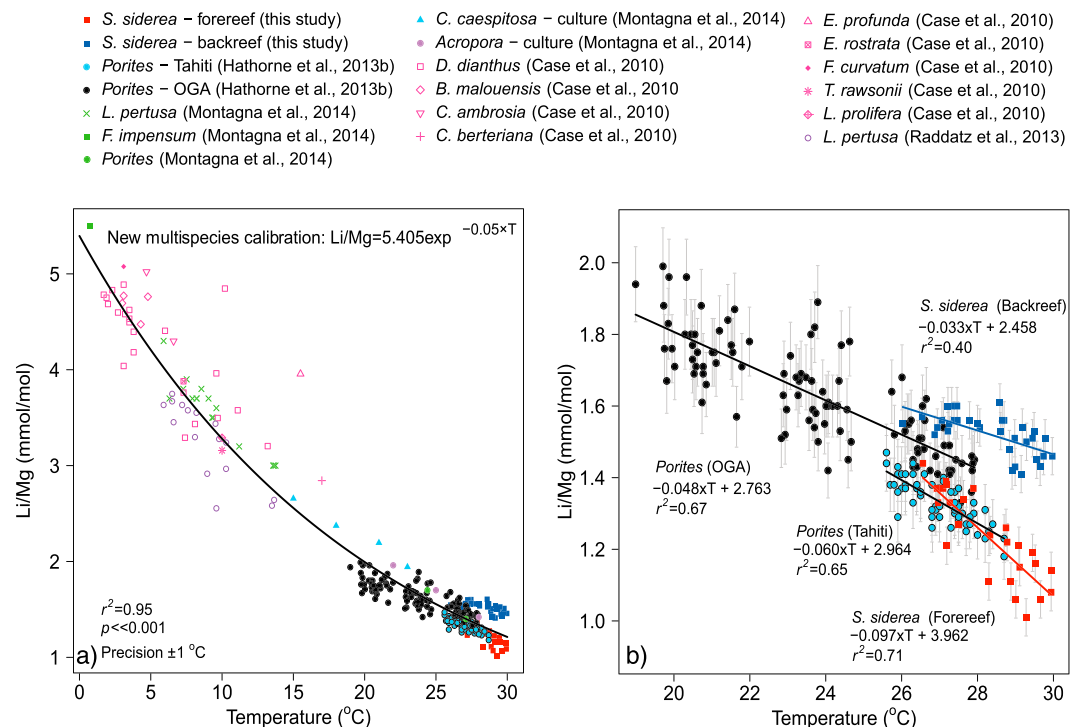


**Figure 5.** (a) Combined Li/Mg-T calibration for a range of coral species at seawater temperatures between  $0^{\circ}C$  and  $30^{\circ}C$ . An exponential regression is used to form the new multispecies calibration. The forereef and backreef calibrations of *S. siderea* from this study are shown by the solid red and blue squares, respectively. (b) Comparison of the linear relationships of the Li/Mg ratios of the tropical species *Porites* (closed circles) and forereef and backreef *S. siderea* (closed squares). The  $2\sigma$  external precision error bars are shown.

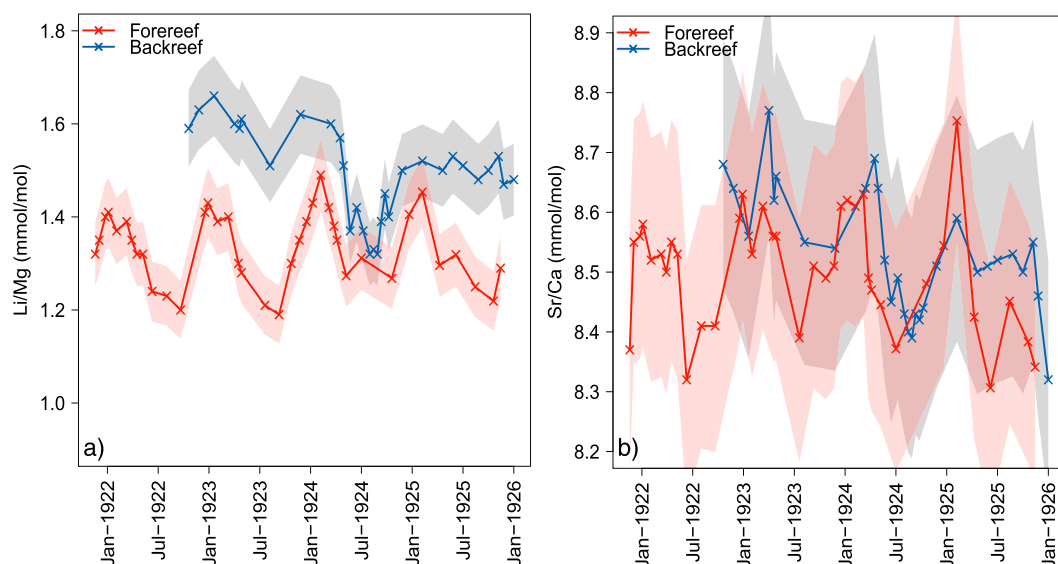


**Figure 6.** Downcore (a) Li/Mg ratios and (b) Sr/Ca ratios of FR-12 forereef (red) and BR-06 backreef (blue) *S. siderea* samples from years 1921 to 1926. The error envelopes (pink and grey) represent the  $2\sigma$  external precision. HadISST data are shown in black for comparison (black line).

winter Sr/Ca-SSTs are  $1.9^{\circ}\text{C}$  greater than HadISST (Table 4). In both of the reef zones, however, the root-mean-square error (RMSE) is within the uncertainties of the single proxy calibrations (Tables 2 and 4).

The multiproxy calibrations yield temperature records similar to those predicted by the single-proxy calibrations (Table 4). However, the multiproxy calibrations have lower reconstruction uncertainties (Table 3), and therefore predict temperatures that match more closely between reef zones and between reconstructed SSTs and HadISST (Table 4), particularly with respect to the backreef reconstruction, albeit with a tendency to reconstruct lower amplitude seasonal variations (Figures 7b and 7d). The multiproxy SSTs in the backreef reduce the differences from HadISST to  $\leq 1.6^{\circ}\text{C}$  (Table 4). As with the single proxy reconstructions, the RMSE of the multiproxy-based means are within the uncertainty of the calibration when comparing to the HadISST data set.

## 4. Discussion

### 4.1. Li/Mg-SST, Sr/Ca-SST, and Multiproxy SST Models in *S. siderea*

Both Sr/Ca and Li/Mg ratios exhibit a well-correlated inverse relationship with temperature in both reef zones (Figures 3 and 4). Within the same reef zone, the slopes of both calibrations are within error of each other, suggesting that both proxies have similar temperature sensitivities. Both Li/Mg and Sr/Ca are also more strongly correlated with temperature in the forereef coral (Table 2). These differences arise even though both reef zones experienced similar temperature histories according to the available observational data (Figure 1b), suggesting that at least one other factor must be influencing both SST proxies.

Geographic differences in Sr/Ca-SST calibrations have been reported before. Several studies have ascribed such variability to the influence of other variables such as seawater pH [Tanaka *et al.*, 2015], seawater Sr/Ca composition [de Villiers *et al.*, 1994], extension rate [de Villiers *et al.*, 1994], and calcification rate [Ferrier-Pagès *et al.*, 2002; Kuffner *et al.*, 2012], which individually, or in combination, influence variation in the extent of Rayleigh fractionation and elemental incorporation in coral aragonite at a particular site. We confirm here that Li/Mg also exhibits a geographically dependent SST calibration, and because the  $K_D$  for Li/Mg is close to unity, we cannot ascribe this variation to Rayleigh fractionation. The influence of a non-SST driver on Li, Mg, and Sr uptake in the backreef coral may also be indicated by (i) the generally poor agreement between Li/Mg-SST, Sr/Ca-SST, and HadISST for the backreef in the years 1922–1926 (Figure 7c), which contrasts the good agreement found for the forereef reconstruction (Figure 7a), and (ii) a lack of evidence for coral bleaching or mortality that would be expected to occur if SSTs were in excess of  $32^{\circ}\text{C}$  as suggested by backreef SST reconstructions (Figure 7). Potential differences between seawater pH of the backreef and forereef may partly explain the spatial variability in SST

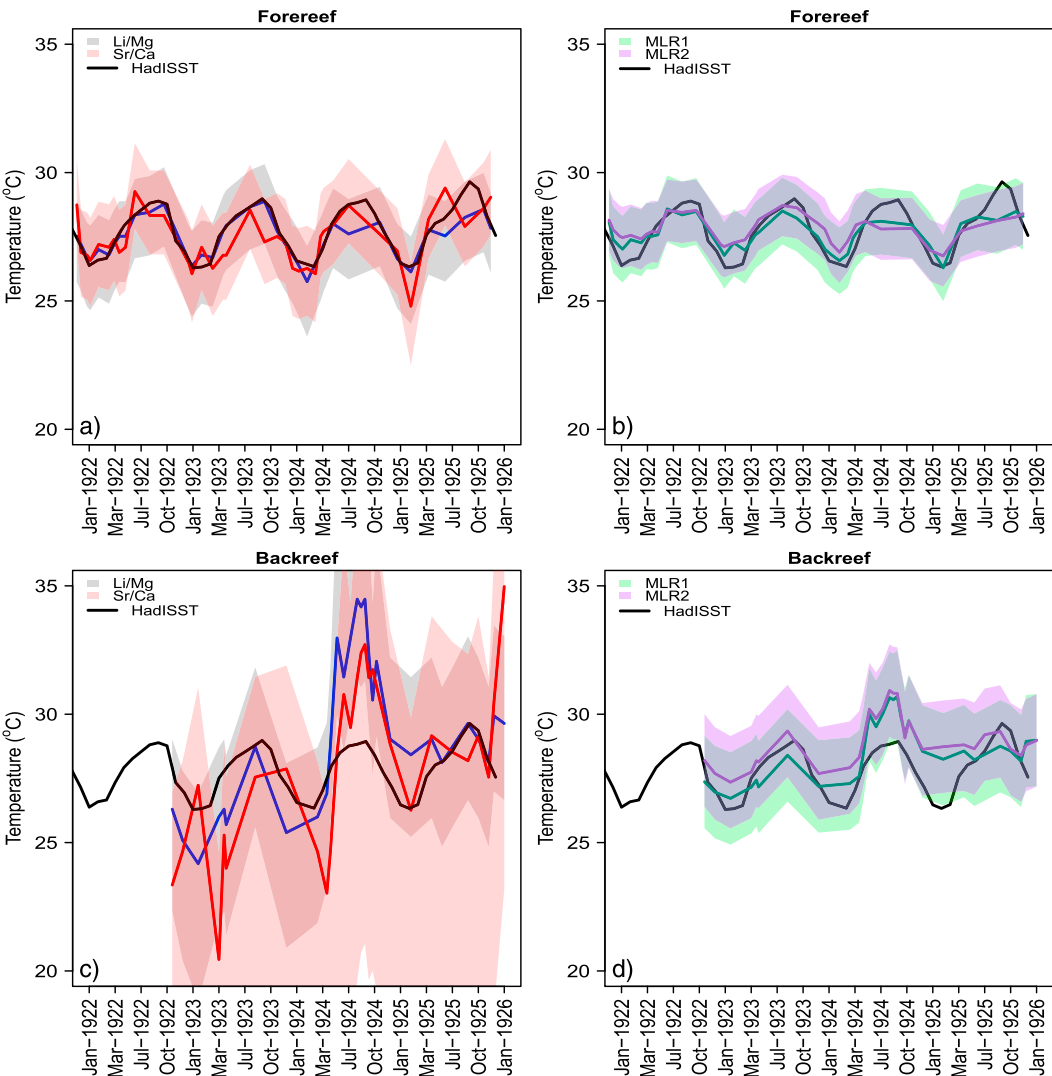


**Figure 7.** Sea surface temperature (SST) reconstructions from 1921 to 1926 using the site-specific *S. siderea* Li/Mg and Sr/Ca-SST proxies and multiproxy calibrations. The blue line shows the Li/Mg-SST, the red line shows the Sr/Ca-SST, the green line shows the combined Li/Mg-Sr/Ca-SST, and the purple line shows the combined Li/Ca-Sr/Ca-Mg/Ca-SST. The shaded regions show the precision estimates derived from the 95% prediction intervals of the linear regressions. HadISST data are also shown for comparison (black line).

**Table 4.** Mean Summer, Winter, and Overall Sea Surface Temperatures Based on the Li/Mg, Sr/Ca, and Multiproxy Reconstructions for Both the Forereef and Backreef<sup>a</sup>

Method	Mean SST (°C)	RMSE HadISST	Summer Mean (°C)	RMSE HadISST	Winter Mean (°C)	RMSE HadISST
HadISST	27.7 (±0.3)		28.9 (±0.2)		26.7 (±0.2)	
FR Li/Mg	27.4 (±0.3)	1.08	28.4 (±0.6)	0.76	26.8 (±0.3)	0.46
FR Sr/Ca	27.4 (±0.3)	1.27	28.2 (±0.6)	0.90	26.7 (±0.6)	0.96
FR MLR1	27.6 (±0.2)	0.97	28.3 (±0.2)	0.68	27.1 (±0.3)	0.68
FR MLR2	27.8 (±0.2)	0.96	28.4 (±0.4)	0.69	27.4 (±0.3)	0.86
BR Li/Mg	29.2 (±1.0)	3.03	32.2 (±2.3)	4.14	27.4 (±1.8)	2.40
BR Sr/Ca	28.1 (±1.2)	3.41	30.7 (±1.7)	2.76	28.6 (±2.5)	3.89
BR MLR1	28.6 (±0.4)	1.62	29.8 (±0.9)	1.44	27.9 (±0.7)	1.69
BR MLR2	29.0 (±0.4)	1.76	30.2 (±0.6)	1.52	28.2 (±0.5)	1.84

<sup>a</sup>Errors are reported as 2 standard errors. The RMSE of the reconstructed mean against the mean HadISST is also shown.

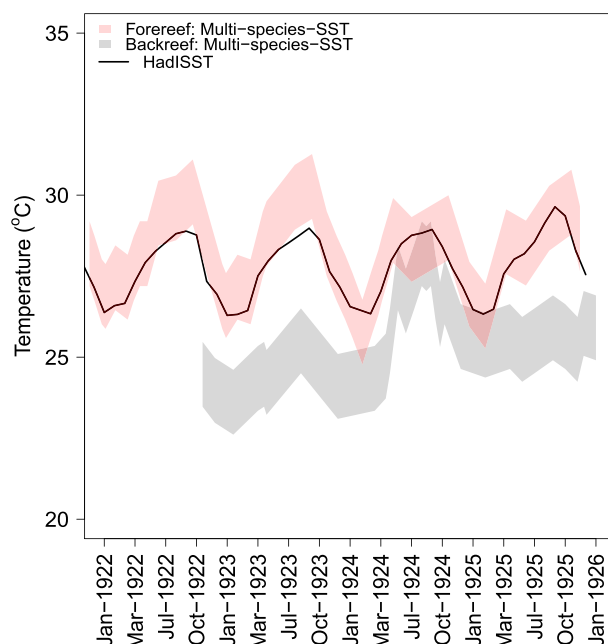


**Figure 8.** Sea surface temperature (SST) reconstructions from 1921 to 1926 using the updated multispecies Li/Mg-SST proxy. The error envelopes show the absolute SST precision estimates derived from the 2 standard error of the exponential calibration slope. Forereef SST reconstructions (red) and backreef SST reconstructions (grey) are compared against the HadISST data (solid black line).

calibrations [Tanaka *et al.*, 2015]. Furthermore, calibrating the SST proxies when extension rates of backreef corals were higher than forereef corals (since the 1990s [Castillo *et al.*, 2011]) and applying them to samples from a time when the extension rates of forereef and backreef corals were more similar may also be at least partially responsible for the breakdown of the Li/Mg- and Sr/Ca-SST proxies. Our assessment of the importance of parameters such as these on Li/Mg and Sr/Ca ratios is the focus of a future study. Nonetheless, part of the degraded performance of both proxies in the backreef coral is also likely due to the size of the analytical uncertainty (Table 1) and the shallower relationship between the measured ratio and observed temperature (Table 2). Indeed, the RMSE between Li/Mg-SST and Sr/Ca-SST with HadISST in the backreef is similar to the calibration uncertainty suggesting that the predictive capabilities of these proxies would improve if the analytical uncertainties were reduced (Tables 2 and 4).

Applying the multiproxy calibrations to the downcore data improved the precision of the reconstructions and reduced the extreme values recorded by the Li/Mg- and Sr/Ca-based SSTs in the backreef (Figure 7d). This improvement is likely, at least in part, a consequence of the increased precision resulting from using multiple variables (Table 3). Despite this advantage, the multiproxy models still fail to predict the expected wintertime temperatures in the backreef that are expected based upon the forereef reconstructions or the HadISST data (Table 4). This result suggests that although the multiproxy calibrations offer some improvement over the single-proxy models in the backreef (Table 4), combining the proxies does not completely eliminate the errors evident in the single-proxy models (Figure 7d and section 3.3).

#### 4.2. Assessment of Tropical Coral Li/Mg-SST Calibrations

Previous studies have highlighted that Li/Mg ratios exhibit a similar inverse relationship with temperature across multiple coral species and over a temperature range of 0°C to 30°C (see references in Figure 5a). Although the forereef and backreef coral data generally agree with this overall trend (Figure 5a), detailed inspection reveals that both of the new Li/Mg-SST calibrations are slightly offset from the multispecies calibration, further highlighting the influence of a non-SST-based parameter(s) in driving Li/Mg variability (Figure 5b). Similar, but more subtle variations are also evident in *Porites* [Hathorne *et al.*, 2013b]. The slope of the backreef *S. siderea* (−0.033) is almost half that of both the Tahiti and OGA *Porites* data (−0.060 and −0.048, respectively [Hathorne *et al.*, 2013b]), which are themselves almost half that of the forereef *S. siderea* (−0.097; Figure 5b). This suggests that although there is a clear overall relationship between temperature and coral Li/Mg, the divergence of tropical corals from a single calibration highlights that accurate reconstructions still require site- and species-specific calibrations.

To demonstrate the importance of these site- and species-specific calibrations, the multispecies calibration (Figure 5a and equation (1)) was applied to the downcore Li/Mg ratios and reconstructed temperatures are compared to historic HadISST data (Figure 8). The forereef SSTs reconstructed by using the multispecies calibration (equation (1)) are mostly within error of HadISST, with the exception of the 1922 and 1923 summertime SSTs, which are slightly overestimated. However, backreef SSTs reconstructed in the same manner are consistently lower than HadISST temperatures (Figure 8).

## 5. Conclusions and Recommendations

The sea surface temperature calibrations presented here demonstrate that the Li/Mg-SST proxy is equal to, and in some locations, more precise than the more commonly used Sr/Ca-SST proxy for the species *S. siderea* ( $\pm 1.5^{\circ}\text{C}$  versus  $\pm 1.6^{\circ}\text{C}$  in forereef coral FR-12). By combining elemental ratios to form multiproxy SST calibrations, the precision of the SST reconstructions is further improved. Both single elemental ratios (Sr/Ca and Li/Mg) in the backreef locality were found to be less sensitive to temperature, indicating that a secondary, non-SST variable impacts the uptake of these elements in the skeletal aragonite of *S. siderea* in these environments. As a test of reliability, reconstructed temperatures from 1921 to 1926 in both reef zones were compared to the HadISST record. Reconstructed forereef temperatures using the Li/Mg, Sr/Ca and the combined Li/Mg-Sr/Ca and Li/Ca-Mg/Ca-Sr/Ca proxies were not significantly different from each other, and these SSTs were also found to be within error of the HadISST data. Reconstructed temperatures from the backreef were found to be substantially offset from forereef reconstructions and HadISST data, and recorded anomalously high temperatures approaching  $35^{\circ}\text{C}$  (presumably damaging or fatal to coral), confirming their inaccuracy.

These results demonstrate that in some regions, Li/Mg, when used in isolation or in combination with other elemental ratios as part of a multiproxy approach, is a suitable addition to the temperature reconstruction tool-box of *S. siderea*. It remains unclear why our backreef reconstructions using Sr/Ca and/or Li/Mg are compromised, but this may be related to spatial variability in linear extension rates of *S. siderea* documented in this region, and for these samples in particular, by Castillo *et al.* [2011]. Nonetheless, in light of the more precise SST reconstructions that result from the multiproxy calibrations, we encourage their use over single elemental ratio proxies as a means of quantifying local surface ocean warming from elemental ratios within the coral *S. siderea*. While further investigation of the non-SST controls on SST proxies, such as Li/Mg, is required, it is clear from our study that the most reliable coral-based reconstructions of sea surface temperatures are obtained through combining multiproxy records that are calibrated in the same region to which they are applied.

## Acknowledgments

This research was funded by the Natural Environment Research Council UK (Studentship number NE/K500926/1 to S.E.F.) and the National Oceanography Centre Southampton Graduate School. The collection and preparation of the coral cores were funded by NOAA award NA13OAR4310186 (to J.B.R. and K.D.C.) and NSF award 1437371 (to J.B.R.). Permits for collection and export were granted by the Belize Fisheries Department, Government of Belize. Reynolds data sets are freely available from [www.nhc.noaa.gov/sst/](http://www.nhc.noaa.gov/sst/) and listed in the supplementary Table S1. Hadley Centre's HadISST1 data are freely available from KNMI Climate Explorer (<http://climexp.knmi.nl/>) and are also listed in Tables S1 and S5. Supporting analytical data are included as three tables in a supporting information file, and data from other coral studies are cited and referred to in the reference list. Many thanks are extended to the B-team, Andy Milton, and Matt Cooper for their assistance in the clean chemistry and plasma labs. We are also grateful to Caroline Lear and Anabel Morte-Ródenas of Cardiff University for their supplying the multielement bracketing standard. We thank the anonymous reviewers for their constructive comments which improved this manuscript.

## References

- Al-Ammar, A. S., R. K. Gupta, and R. M. Barnes (2000), Elimination of boron memory effect in inductively coupled plasma-mass spectrometry by ammonia gas injection into the spray chamber during analysis, *Spectrochim. Acta, Part B*, 55, 629–635.
- Alibert, C., and M. T. McCulloch (1997), Strontium/calcium ratios in modern *Porites* corals from the Great Barrier Reef as a proxy for sea surface temperature: Calibration of the thermometer and monitoring of ENSO, *Paleoclimatology*, 12, 345–363, doi:10.1029/97PA00318.
- Allison, N., A. A. Finch, M. Newville, and S. R. Sutton (2005), Strontium in coral aragonite: 3. Sr coordination and geochemistry in relation to skeletal architecture, *Geochim. Cosmochim. Acta*, 69(15), 3801–3811.
- Alpert, A. E., A. L. Cohen, D. W. Oppo, T. M. DeCarlo, J. M. Gove, and C. W. Young (2016), Comparison of equatorial Pacific sea surface temperature variability and trends with Sr/Ca records from multiple corals, *Paleoclimatology*, 31, 252–265, doi:10.1002/2015PA002897.
- Anand, P., H. Elderfield, and M. H. Conte (2003), Calibration of Mg/Ca thermometry in planktonic foraminifera from a sediment trap time series, *Paleoclimatology*, 18(2), 1050, doi:10.1029/2002PA000846.
- Anderson, D. M., E. M. Mauk, E. R. Wahl, C. Morrill, A. J. Wagner, D. Easterling, and T. Rutishauser (2013), Global warming in an independent record of the past 130 years, *Geophys. Res. Lett.*, 40, 189–193, doi:10.1029/2012GL054271.
- Barker, S., M. Greaves, and H. Elderfield (2003), A study of cleaning procedures used for foraminiferal Mg/Ca paleothermometry, *Geochim. Geophys. Geosyst.*, 4(9), 8407, doi:10.1029/2003GC000559.
- Beck, J. W., R. L. Edwards, E. Ito, F. W. Taylor, J. Recy, F. Rougerie, P. Joannot, and C. Henin (1992), Sea-surface temperature from coral skeletal strontium/calcium ratios, *Science*, 257(5070), 644–647.
- Brassell, S. C., G. Eglinton, I. T. Marlowe, U. Pflaumann, and M. Sarnthein (1986), Molecular stratigraphy: A new tool for climatic assessment, *Nature*, 320, 129–133.
- Caroselli, E., F. Zaccanti, G. Mattioli, G. Falini, O. Levy, Z. Dubinsky, and S. Goffredo (2012), Growth and demography of the solitary scleractinian coral *Leptopsammia pruvoti* along a sea surface temperature gradient in the Mediterranean Sea, *PLoS One*, 7(6), e37848.
- Case, D. H., L. F. Robinson, M. E. Auro, and A. C. Gagnon (2010), Environmental and biological controls on Mg and Li in deep-sea scleractinian corals, *Earth Planet. Sci. Lett.*, 300, 215–225.
- Castillo, K. D., and F. P. Lima (2010), Comparison of in situ and satellite-derived (MODIS-Aqua/Terra) methods for assessing temperatures on coral reefs, *Limnol. Oceanogr. Methods*, 8(3), 107–117.
- Castillo, K. D., J. B. Ries, and J. M. Weiss (2011), Declining coral skeletal extension for forereef colonies of *Siderastrea siderea* on the Mesoamerican Barrier Reef System, Southern Belize, *PLoS One*, 6(2), e14615.
- Castillo, K. D., J. B. Ries, J. M. Weiss, and F. P. Lima (2012), Decline of forereef corals in response to recent warming linked to history of thermal exposure, *Nat. Clim. Change*, 2(10), 756–760.
- Cohen, A. L., G. D. Layne, S. R. Hart, and P. S. Lobel (2001), Kinetic control of skeletal Sr/Ca in a symbiotic coral: Implications for the paleotemperature proxy, *Paleoclimatology*, 16, 20–26, doi:10.1029/1999PA000478.
- Cohen, A. L., K. E. Owens, G. D. Layne, and N. Shimizu (2002), The effect of algal symbionts on the accuracy of Sr/Ca paleotemperatures from coral, *Science*, 296, 331–333.
- Cohen, A. L., G. A. Gaetani, T. Lundälv, B. H. Corliss, and R. Y. George (2006), Compositional variability in a cold-water scleractinian, *Lophelia pertusa*: New insights into “vital effects”, *Geochim. Geophys. Geosyst.*, 7, Q12004, doi:10.1029/2006GC001354.



- Corrège, T. (2006), Sea surface temperature and salinity reconstruction from coral geochemical tracers, *Palaeogeogr. Palaeoclimatol. Palaeoecol.*, **232**, 408–428.
- Cubasch, U., D. Wuebbles, D. Chen, M. C. Facchini, D. Frame, N. Mahowald, and J.-G. Winther (2013), Introduction, in *Climate Change 2013: The Physical Science Basis. Contribution of Working Group I to the Fifth Assessment Report of the Intergovernmental Panel on Climate Change*, edited by T. F. Stocker, pp. 119–158, Cambridge Univ. Press, Cambridge, U. K., and New York.
- DeLong, K. L., J. A. Flannery, C. R. Maupin, R. Z. Poore, and T. M. Quinn (2011), A coral Sr/Ca calibration and replication study of two massive corals from the Gulf of Mexico, *Palaeogeogr. Palaeoclimatol. Palaeoecol.*, **307**, 117–128.
- DeLong, K. L., J. A. Flannery, R. Z. Poore, T. M. Quinn, C. R. Maupin, K. Lin, and C.-C. Shen (2014), A reconstruction of sea surface temperature variability in the southeastern Gulf of Mexico from 1734–2008 CE using cross-dated Sr/Ca records from the coral *Siderastrea siderea*, *Paleoceanography*, **29**, 403–422, doi:10.1002/2013PA002524.
- de Villiers, S., G. T. Shen, and B. K. Nelson (1994), The Sr/Ca-temperature relationship in coralline aragonite: Influence of variability in and skeletal growth parameters, *Geochim. Cosmochim. Acta*, **58**, 197–208.
- Fallon, S. J., M. T. McCulloch, and C. Alibert (2003), Examining water temperature proxies in *Porites* corals from the Great Barrier Reef: A cross-shelf comparison, *Coral Reefs*, **22**, 389–404.
- Felis, T., G. Lohmann, H. Kuhnert, S. J. Lorenz, D. Scholz, J. Pätzold, S. A. Al-Rousan, and S. M. Al-Moghrabi (2004), Increased seasonality in Middle East temperatures during the last interglacial period, *Nature*, **429**, 164–168.
- Felis, T., A. Suzuki, H. Kuhnert, M. Dima, G. Lohmann, and H. Kawahata (2009), Subtropical coral reveals abrupt early-twentieth-century freshening in the western North Pacific Ocean, *Geology*, **37**(6), 527–530.
- Ferrier-Pagès, C., F. Boisson, D. Allemand, and E. Tambutté (2002), Kinetics of strontium uptake in the scleractinian coral *Stylophora pistillata*, *Mar. Ecol. Prog. Ser.*, **245**, 93–100.
- Finch, A. A., and N. Allison (2008), Mg structural state in coral aragonite and implications for the paleoenvironmental proxy, *Geophys. Res. Lett.*, **35**, L08704, doi:10.1029/2008GL033543.
- Gaetani, G. A., and A. L. Cohen (2006), Element partitioning during precipitation of aragonite from seawater: A framework for understanding paleoproxies, *Geochim. Cosmochim. Acta*, **70**, 4617–4634.
- Gaetani, G. A., A. L. Cohen, Z. Wang, and J. Crisius (2011), Rayleigh-based, multi-element coral thermometry: A biomineralization approach to developing climate proxies, *Geochim. Cosmochim. Acta*, **75**, 1920–1932.
- Gagan, M. K., G. B. Dunbar, and A. Suzuki (2012), The effect of skeletal mass accumulation in *Porites* on coral Sr/Ca and  $\delta^{18}\text{O}$  paleothermometry, *Paleoceanography*, **27**, PA1203, doi:10.1029/2011PA002215.
- Gagnon, A. C., J. F. Adkins, D. P. Fernandez, and L. F. Robinson (2007), Sr/Ca and Mg/Ca vital effects correlated with skeletal architecture in a scleractinian deep-sea coral and the role of Rayleigh fractionation, *Earth Planet. Sci. Lett.*, **261**(1–2), 280–295.
- Gagnon, A. C., J. Adkins, and J. Erez (2012), Seawater transport during coral biomineralization, *Earth Planet. Sci. Lett.*, **329–330**, 150–161.
- Gagnon, A. C., J. F. Adkins, J. Erez, J. M. Eiler, and Y. Guan (2013), Sr/Ca sensitivity to aragonite saturation state in cultured subsamples from a single colony of coral: Mechanism of biomineralization during ocean acidification, *Geochim. Cosmochim. Acta*, **105**, 240–254.
- Glenn, E., D. Comarazamy, J. E. González, and T. Smith (2015), Detection of recent regional sea surface temperature warming in the Caribbean and surrounding region, *Geophys. Res. Lett.*, **42**, 6785–6792, doi:10.1002/2015GL065002.
- Hathorne, E. C., et al. (2013a), Interlaboratory study for coral Sr/Ca and other element/Ca ratio measurements, *Geochem. Geophys. Geosyst.*, **14**, 3730–3750, doi:10.1002/ggge.20230.
- Hathorne, E. C., T. Felis, A. Suzuki, H. Kawahata, and G. Cabioch (2013b), Lithium in the aragonite skeletons of massive *Porites* corals: A new tool to reconstruct tropical sea surface temperatures, *Paleoceanography*, **28**, 143–152, doi:10.1029/2012PA002311.
- Henehan, M. J., J. W. Rae, G. L. Foster, J. Erez, K. C. Prentice, M. Kucera, H. C. Bostock, M. A. Martínez-Botí, J. A. Milton, and P. A. Wilson (2013), Calibration of the boron isotope proxy in the planktonic foraminifera *Globigerinoides ruber* for use in palaeo- $\text{CO}_2$  reconstruction, *Earth Planet. Sci. Lett.*, **364**, 111–122.
- Ip, Y. K., and A. L. Lim (1991), Are calcium and strontium transported by the same mechanism in the hermatypic coral *Galaxea fascicularis*, *J. Exp. Biol.*, **159**, 507–513.
- Kennedy, J. J., N. A. Rayner, R. O. Smith, D. E. Parker, and M. Saunby (2011), Reassessing biases and other uncertainties in sea surface temperature observations measured in situ since 1850: 2. Biases and homogenization, *J. Geophys. Res.*, **116**, D14104, doi:10.1029/2010JD015220.
- Kuffner, I. B., P. L. Jokiel, K. S. Rodgers, A. J. Andersson, and F. T. Mackenzie (2012), An apparent “vital effect” of calcification rate on the Sr/Ca temperature proxy in the reef coral *Montipora capitata*, *Geochem. Geophys. Geosyst.*, **13**, Q08004, doi:10.1029/2012GC004128.
- Marriott, C. S., G. M. Henderson, N. S. Belshaw, and A. W. Tudhope (2004a), Temperature dependence of  $\delta^7\text{Li}$ ,  $\delta^{44}\text{Ca}$  and Li/Ca during growth of calcium carbonate, *Earth Planet. Sci. Lett.*, **222**(2), 615–624.
- Marriott, C. S., G. M. Henderson, R. Crompton, M. Staubwasser, and S. Shaw (2004b), Effect of mineralogy, salinity, and temperature on Li/Ca and Li isotope composition of calcium carbonate, *Chem. Geol.*, **212**(1–2), 5–15.
- Maupin, C. R., T. M. Quinn, and R. B. Halley (2008), Extracting a climate signal from the skeletal geochemistry of the Caribbean coral *Siderastrea siderea*, *Geochem. Geophys. Geosyst.*, **9**, Q12012, doi:10.1029/2008GC002106.
- McCulloch, M. T., M. K. Gagan, G. E. Mortimer, A. R. Chivas, and P. J. Isdale (1994), A high-resolution Sr/Ca and  $\delta^{18}\text{O}$  coral record from the Great Barrier Reef, Australia, and the 1982–1983 El Niño, *Geochim. Cosmochim. Acta*, **58**(12), 2747–2754.
- Meibom, A., et al. (2006), Vital effects in coral skeletal composition display strict three-dimensional control, *Geophys. Res. Lett.*, **33**, L11608, doi:10.1029/2006GL025968.
- Mitsuguchi, T., E. Matsumoto, O. Abe, T. Uchida, and P. J. Isdale (1996), Mg/Ca thermometry in coral skeletons, *Science*, **274**(5289), 961–963.
- Mitsuguchi, T., P. X. Dang, H. Kitagawa, T. Uchida, and Y. Shibata (2008), Coral Sr/Ca and Mg/Ca records in Con Dao Island off the Mekong Delta: Assessment of their potential for monitoring ENSO and East Asian monsoon, *Global Planet. Change*, **63**(4), 341–352.
- Montagna, P., et al. (2014), Li/Mg systematics in scleractinian corals: Calibration of the thermometer, *Geochim. Cosmochim. Acta*, **132**, 288–310.
- Ni, Y. (2006), Evaluation of boron isotopes and trace abundances in planktonic foraminifers as palaeo-oceanographic proxies, PhD thesis, 217 pp., Univ. of Bristol.
- Ni, Y., G. L. Foster, T. Bailey, T. Elliott, D. N. Schmidt, P. Pearson, B. Haley, and C. Coath (2007), A core top assessment of proxies for the ocean carbonate system in surface-dwelling foraminifers, *Paleoceanography*, **22**, PA3212, doi:10.1029/2006PA001337.
- Okai, T., A. Suzuki, H. Kawahata, S. Terashima, and N. Imai (2002), Preparation of a new geological survey of Japan Geochemical Reference Material: Coral JcP-1, *Geostand. NewsL.*, **26**(1), 95–99.
- Raddatz, J., et al. (2013), Stable Sr-isotope, Sr/Ca, Mg/Ca, Li/Ca and Mg/Li ratios in the scleractinian cold-water coral *Lophelia pertusa*, *Chem. Geol.*, **352**, 143–152.

- Rayner, N. A., D. E. Parker, E. B. Horton, C. K. Folland, L. V. Alexander, and D. P. Rowell (2003), Global analyses of sea surface temperature, sea ice, and night marine air temperature since the late nineteenth century, *J. Geophys. Res.*, **108**(D14), 4407, doi:10.1029/2002JD002670.
- Rayner, N. A., P. Brohan, D. Parker, C. Folland, J. Kennedy, M. Vanicek, T. Ansell, and S. Tett (2006), Improved analyses of changes and uncertainties in sea surface temperature measured in situ since the mid-nineteenth century: The HadSST2 dataset, *J. Clim.*, **19**(3), 446–469.
- R Development Core Team (2013), *R: A Language and Environment for Statistical Computing*, R Found. for Stat. Comput., Vienna [Available at <http://www.R-project.org/>].
- Reynaud, S., C. Ferrier-Pagès, A. Meibom, S. Mostefaoui, R. Mortlock, R. Fairbanks, and D. Allemand (2007), Light and temperature effects on Sr/Ca and Mg/Ca ratios in the scleractinian coral *Acropora* sp., *Geochim. Cosmochim. Acta*, **71**(2), 354–362.
- Reynolds, R. W., T. M. Smith, C. Liu, D. B. Chelton, K. S. Casey, and M. G. Schlax (2007), Daily high-resolution-blended analyses for sea surface temperature, *J. Clim.*, **20**(22), 5473–5496.
- Rhein, M., et al. (2013), Observations: Ocean, in *Climate Change 2013: The Physical Science Basis. Contribution of Working Group I to the Fifth Assessment Report of the Intergovernmental Panel on Climate Change*, pp. 255–316, Cambridge Univ. Press, Cambridge, U. K.
- Rosenheim, B. E., P. K. Swart, S. R. Thorrold, P. Willenz, L. Berry, and C. Latkoczy (2004), High-resolution Sr/Ca records in sclerosponges calibrated to temperature in situ, *Geology*, **32**(2), 145–148.
- Rosenthal, Y., M. P. Field, and R. M. Sherrell (1999), Precise determination of element/calcium ratios in calcareous samples using sector field inductively coupled plasma mass spectrometry, *Anal. Chem.*, **71**, 3248–3253.
- Saenger, C., A. L. Cohen, D. W. Oppo, and D. Hubbard (2008), Interpreting sea surface temperature from strontium/calcium ratios in *Montastrea* corals: Link with growth rate and implications for proxy reconstructions, *Paleoceanography*, **23**, PA3102, doi:10.1029/2007PA001572.
- Schouten, S., E. C. Hopmans, E. Schefuss, and J. S. Sinninghe Damsté (2002), Distributional variations in marine crenarchaeotal membrane lipids: A new tool for reconstructing ancient sea water temperatures?, *Earth Planet. Sci. Lett.*, **204**, 265–274.
- Shannon, R. t. (1976), Revised effective ionic radii and systematic studies of interatomic distances in halides and chalcogenides, *Acta Crystallogr., Sect. A*, **32**(5), 751–767.
- Sinclair, D. J., and M. J. Risk (2006), A numerical model of trace-element coprecipitation in a physicochemical calcification system: Application to coral biomineralization and trace-element ‘vital effects’, *Geochim. Cosmochim. Acta*, **70**(15), 3855–3868.
- Smith, T. M., R. W. Reynolds, T. C. Peterson, and J. Lawrimore (2008), Improvements to NOAA’s historical merged land–ocean surface temperature analysis (1880–2006), *J. Clim.*, **21**, 2283–2296.
- Swart, P. K., H. Elderfield, and M. J. Greaves (2002), A high-resolution calibration of Sr/Ca thermometry using the Caribbean coral *Montastrea annularis*, *Geochim. Geophys. Geosyst.*, **3**(11), 8402, doi:10.1029/2002GC000306.
- Tambutté, S., M. Holcomb, C. Ferrier-Pagès, S. Reynaud, É. Tambutté, D. Zoccola, and D. Allemand (2011), Coral biomineralization: From the gene to the environment, *J. Exp. Mar. Biol. Ecol.*, **408**(1–2), 58–78.
- Tanaka, K., M. Holcomb, A. Takahashi, H. Kurihara, R. Asami, R. Shinjo, K. Sowa, K. Rankenburg, T. Watanabe, and M. McCulloch (2015), Response of *Acropora digitifera* to ocean acidification: Constraints from  $\delta^{11}\text{B}$ , Sr, Mg, and Ba compositions of aragonitic skeletons cultured under variable seawater pH, *Coral Reefs*, **34**(4), 1139–1149.
- Tierney, J. E., N. J. Abram, K. J. Anchukaitis, M. N. Evans, C. Giry, K. H. Kilbourne, C. P. Saenger, H. C. Wu, and J. Zinke (2015), Tropical sea surface temperatures for the past four centuries reconstructed from coral archives, *Paleoceanography*, **30**, 226–252, doi:10.1002/2014PA002717.
- Watson, E. B. (1996), Surface enrichment and trace-element uptake during crystal growth, *Geochim. Cosmochim. Acta*, **60**(24), 5013–5020.
- Weber, J. N. (1973), Incorporation of strontium into reef coral skeletal carbonate, *Geochim. Cosmochim. Acta*, **37**(9), 2173–2190.